PRAMANA
— journal of
physics

Vol. 43, No. 6,
December 1994
pp. 495–502

Vibrationally elastic $e^- - H_2O$ scattering at intermediate energies

K N JOSHIPURA, MINAXI VINODKUMAR* and P M PATEL*
Department of Physics, Sardar Patel University, Vallabh Vidyanagar 388 120, India
*V.P. & R.P.T.P. Science College, Vallabh Vidyanagar 388 120, India

MS received 14 December 1993; revised 13 April 1994

Abstract. Vibrationally elastic total cross-sections of e^-–H_2O scattering are calculated at intermediate energies $E_i = 10$–300 eV. The interaction potentials are treated in spherical models. The dipole rotational excitation, which is significant but not dominant above 10 eV, is treated incoherently. Effects of electronic excitation-ionization, significant above 30 eV or so, are considered through a complex optical potential. A dynamically distorted charge-density is employed to calculate the imaginary part of the complex potential. Comparisons are made with recent theoretical and experimental data. The mutual agreement is better in total cross-sections than in differential cross-sections.

Keywords. Elastic and inelastic electron-scattering; optical potential, total cross-sections.

PACS No. 34·80

1. Introduction

This paper deals with some of the theoretical aspects of the scattering of electrons by water molecules. This has been recently investigated by Itikawa and co-workers and by others [1–3]. We confine ourselves mainly to total cross-sections of e^-–H_2O scattering, for which experimental data have been given by Johnstone and Newell [4], Sueoka *et al* [5] and others. All these workers have also emphasized the importance of the study of e^-–H_2O scattering.

The interaction of an electron with a molecule like H_2O is in general nonspherical. Rotational excitation of the molecule due to the long range dipole potential dominates the e^-–H_2O total cross-sections at low energies. At intermediate and high energies, short range interactions become more significant. At such energies the total e^-–H_2O cross-section can be calculated by assuming the molecule to be spherical and the only important nonspherical effect, that of the dipole rotation, may be incorporated incoherently [3]. We have presently adopted this approach to calculate the total e^-–H_2O cross-sections at intermediate energies. $E_i = 10$–300 eV. Jain [3] calculated these cross-sections by starting with a polarized target charge-density to generate the spherical complex optical potential. Now, the target charge-polarization is a dynamic (energy-dependent) phenomenon, hence we have presently obtained the polarized part of the charge-density through a dynamic polarization potential as well as through its asymptotic form. On the other hand Okamoto *et al* [1] have considered the static (unperturbed) charge-density in their calculations at $E_i = 6 - 50$ eV. They made no allowance for the electronic excitation–ionization channels in their calculations. They

have given a theoretical forward-scattering correction to the experimental total e^-–H_2O cross-sections.

We have employed complex optical potential to calculate the total (elastic + inelastic) cross-sections Q_T^S, within a spherical charge-density, distorted by a dynamic as well as static polarization potential. The nonspherical contribution Q_T^{NS} to the total cross-section, corresponding to rotational excitation is treated separately in the point dipole first Born approximation (PDFBA), following Itikawa [6]. We also examine the overall effect of electronic excitation and ionization channels on elastic e^-–H_2O scattering. Our total as well as differential cross-sections are compared with the recent theoretical and experimental data. The differences in the present results, arising out of (a) unperturbed and perturbed target charge density, and, (b) real and complex potential, are discussed.

2. Theory

Considering the incident electron energies to be intermediate and high, we write the total e^-–H_2O scattering cross-section Q_{tot} as an incoherent sum of the spherical and nonspherical contributions in the following manner

$$Q_{tot} = Q_T^S + Q_T^{NS} \tag{1}$$

Okamato *et al* [1] calculated the total cross-sections in two ways viz. (i) by starting with the complete nonspherical real potential and (ii) by starting with real spherical potential and adding the dipole correction, as in (1). The difference between their two calculations is significant at low energies, roughly below 30 eV. Thus in the present energy range the incoherent approach of (1) is quite suitable.

Now the spherical contribution Q_T^S to the total cross-section (1) is obtained here by starting with an accurate charge-density $\rho_0(r)$ of H_2O, given by Katase *et al* [7]. We represent the e^-–H_2O system by a complex, spherical, energy-dependent optical potential,

$$V_{opt}(r, E_i) = V_{st}(r) + V_{ex}(r, E_i) + V_{pol} + iV_{abs}(r, E_i) \tag{2}$$

where V_{st} is the static potential obtained directly from the static charge-density $\rho_0(r)$. The exchange potential V_{ex} is obtained following the free-electron-gas-exchange model of Hara [8]. For the absorption potential V_{abs} we have adopted the quasi-free Pauli-blocking model given by Truhlar and coworkers [9]. The polarization effects (represented by V_{pol} in (2)) are adequately described, at intermediate energies, by the correlation-polarization potential (see [10, 11]). Towards high energies ($E_i \geqslant 80$ eV here) we have adopted for V_{pol}, a dynamic polarization potential,

$$V_{dp}(r, E_i) = -\frac{1}{2}\frac{\alpha_0 \cdot r^2}{(r^2 + r_c^2)^3} \tag{3}$$

with

$$r_c = 0{\cdot}375k/\Delta$$

here α_0 and Δ are respectively, the average spherical polarizability and the average excitation energy of the target molecule. Further, k is the incident momentum (in a.u.). In (3) a shorter-range term varying asymptotically as r^{-6} may be added, but

that requires a reliable value of the quadrupole polarizability of the molecule. Moreover, the extra term would be ineffective in view of (7) to follow. Now, the incident electron perturbs the target charge distribution, hence the exchange and the absorption potentials (effective near the target) must be derived from a polarized (rather static) charge-density. We have presently calculated the polarized part of the charge-density, denoted by $\rho_{pol}(r, E_i)$, from the dynamic polarization potential $V_{dp}(r, E_i)$, through the Poisson equation,

$$\nabla^2 V_{pol}(r, E_i) = -4\pi\rho_{pol}(r, E_i). \tag{4}$$

Using (3) and (4), the dynamic correction to the charge-density is,

$$\rho_{pol}(r, E_i) = \frac{1}{4\pi}\left[\frac{3\alpha_0}{(r^2+r_c^2)^3} - \frac{21\alpha_0 r^2}{(r^2+r_c^2)^4} + \frac{24\alpha_0 r^4}{(r^2+r_c^2)^5}\right]. \tag{5}$$

If we start with the static asymptotic form $-\alpha_0/2r^4$ of the polarization potential and use the Poisson equation, we obtain the static-correction to the charge-density as $\Delta\rho = 3\alpha_0/2\pi r^6$.

Thus, we introduce the dynamically distorted charge-density,

$$\rho'(r, E_i) = \rho_0(r) + \rho_{pol}(r, E_i). \tag{6a}$$

The statically distorted charge-density would be,

$$\rho(r) = \rho_0(r) + \Delta\rho \tag{6b}$$

Note that unlike $\Delta\rho$, the correction $\rho_{pol} \to 0$ at high energies, making it theoretically more satisfying.

The polarization potential of (3) fails to account for the polarization effect at low energies [11]. Actually at small r, the picture of dipole charge-polarization of the target by an external electron breaks down. For e^-–H_2O scattering this may be the case, typically at $r \leqslant r_{O-H}$, where $r_{O-H} = 1{\cdot}81\ a_0$ is the O–H bond length in H_2O. At such separations the static-exchange potentials dominate, hence we take

$$\rho_{pol}(r, E_i) = 0, \quad \text{if} \quad r \leqslant r_{O-H} \tag{7}$$

Thus, we have considered (6a, 6b) along with (7) to derive the short range potentials.

It is the absorption potential that is modified appreciably by the use of corrections over $\rho_0(r)$. Towards scattering calculations we solved the Schrödinger equation numerically for the real and the imaginary parts of V_{opt} (for details see [12]). The partial wave phase-shifts thus obtained were employed to calculate the total (elastic + inelastic) cross-sections Q_T^S, viz,

$$Q_T^S = Q_{el} + Q_{inel} \tag{8}$$

where, Q_{el} is the total elastic cross-section and Q_{inel} is the total inelastic cross-section, in the complex potential. We have also calculated the purely elastic cross-sections, σ_{el} obtained by setting $V_{abs} = 0$ in (2).

The dipole contribution Q_T^{NS} in (1) was obtained in the PDFBA [6]. This differs somewhat from the expression of Collins and Norcross [13] in that the former treats H_2O as an asymmetric top.

3. Results and discussion

3.1 *Total cross-sections*

We calculated vibrationally elastic e^-–H_2O total cross-sections Q_{tot} at energies $E_i = 10$–300 eV. The polarized charge density, (6) and (7), affects the absorption potential and hence Q_T^S. The total inelastic cross-section Q_{inel} is enhanced by the corrections via (6a) and (6b) in the charge-density, as observed by Jain [3]. However, our correction ρ_{pol} is energy-dependent. This is not so with the calculations of Jain [3], which therefore, overestimate the cross-sections at higher energies. Towards lower energies ($\leqslant 10$ eV) the polarized part of the charge-density has no significant effect on the cross-sections. Table 1 shows our calculated cross-sections Q_{inel} at $E_i = 30$–300 eV. These are compared here mutually in three models for V_{abs}, with (i) no correction over ρ_0, (ii) dynamic correction via (6a), and (iii) static correction via (6b). The quantity of column 3 (table 1) calculated via (6a) is closer to the theoretical ionization cross-sections Q_{ion} (column 5) given by Khare and Meath [14], especially towards high energies. The Q_{inel} including the static correction (column 4, table 1) are higher at high energies, similar to the results of Jain [3]. We have not included the experimental Q_{ion} data of Orient and Srivastava [15] which are still higher at the peak. Recent measurements of Rao [16], not shown, lie somewhat above the

Table 1. Inelastic cross-sections Q_{inel} (in 10^{-16} cm^2) for e^-–H_2O scattering.

	Q_{inel} (present)			
Energy (eV)	No correction (ρ_0 only)	Dynamical correction eq. (6a)	Static correction eq. (6b)	Q_{ion}^* (theoretical)
30	0·33	0·71	0·76	1·1
50	1·07	1·61	1·92	1·9
80	1·62	1·88	2·93	2·1
100	1·76	1·91	3·00	2·1
300	1·31	1·30	1·89	1·4

*Values obtained from the graphical ionization cross-sections of Khare and Meath [14]

Table 2. The present total cross-sections σ_{el}, Q_T^S and Q_{el} (all in 10^{-16} cm^2) for e^-–H_2O scattering, in spherical interactions.

E_i (eV)	Real potential σ_{el}	Complex potential	
		Q_T^S	$Q_{el} = Q_T^S - Q_{inel}$
10	10·2	10·2	10·2
30	7·7	8·3	7·6
50	4·2	5·0	3·9
80	3·6	4·9	3·1
100	2·9	4·3	2·4

values of columns 3 and 5 of table 1 and exhibit a similar energy-dependence. At high energies the entries of columns 2 and 3 tend to agree. This justifies the use of the dynamically perturbed charge-density in our results shown next.

Also investigated presently is the effect of inelastic scattering on elastic scattering at intermediate energies. We calculated the purely elastic cross-sections σ_{el} in a real spherical e^-–H_2O potential. Table 2 exhibits the total cross-sections σ_{el} and the total (elastic + inelastic) cross-sections Q_T^S, together with the total elastic cross-sections, Q_{el} (see (8)). The quantity Q_{inel} represents the overall effect of the electronic (excitation and ionization) channels, at a given energy. It becomes significant above 30 eV and shows a broad peak near 100 eV. Therefore, our values of σ_{el} and Q_T^S (table 2) are close to each other up to about 30 eV only. As E_i increases they differ significantly, with $Q_T^S > \sigma_{el}$, and $\sigma_{el} > Q_{el}$. Thus for $E_i > 30$ eV or so, the effects of electronic channels must be taken into account. This has not been done by Okamoto *et al* [1] in their calculations at $E_i = 6$–50 eV.

Now a quantity that offers a meaningful comparison with experimental data is Q_{tot} of (1). To compare the theoretical results with the experimental ones, we have considered the forward-scattering correction to the measured total cross-sections Q_{tot}, as given theoretically by Okamoto *et al* [1]. The correction ΔQ_{tot}, corresponds to the strong forward scattering by polar molecules like H_2O and is found to fit well with the formula,

$$\Delta Q_{tot}(E_i) = a \cdot (E_i)^{-b} \tag{9}$$

where $a = 30$, and $b = 0{\cdot}75$.

This formula holds good in the present energy range. The (undetected) correction ΔQ_{tot} must be added to the measured total cross-section Q_{tot} for a comparison with the theoretical value at a given energy. Table 3 shows the present values of Q_{tot} along with that of Jain [3]. Also shown are the total cross-sections averaged over the rotational-state distribution at the gas (H_2O) temperature 300 K, i.e. Q (300 K) given by Okamoto *et al* [1]. The last column of table 3 shows the measured cross-sections, with the correction of (9) given in the brackets.

Towards low energies the theoretical values in table 3 are quite similar, indicating (i) a subdued role of the polarized charge-density, and (ii) the dominance of Q_T^{NS} over

Table 3. Total (elastic plus inelastic) cross-sections* Q_{tot} (in 10^{-16} cm^2) for e^-–H_2O scattering.

	Theory			Experimental results
E_i (eV)	Present Q_{tot}	Jain [3]	Okamoto *et al* [1]	(Correction ΔQ_{tot}**)
10	23·1	23·18	23·10	13·89[@] (5·55)
30	13·8	13·08	12·27	11·29[@] (2·46)
50	8·6	10·13	8·35	7·76[@] (1·65)
80	7·4	8·14	—	6·3[£] (1·1)
100	6·2	7·71	—	5·6[£] (0·95)
300	2·8	4·0	—	3·2[£] (0·4)

*See eqn. (1); **See eqn. (9); [@] Johnstone and Newell [4]; [£] Sueoka *et al* [5, 17]

Q_T^S. As E_i increases, we find $Q_T^{NS} < Q_T^S$. Above 30 eV (nearly) Q_{tot} of Jain [3] are higher than ours because of his energy independent ρ_{pol}. At such energies, the cross-sections of Okamoto *et al* [1] are somewhat lower, mainly because of their neglect of the inelastic electronic channels.

Various experiments done so far on total $e^- - H_2O$ cross-sections differ from each other as well as from the corresponding theories also. Johnstone and Newell [4] integrated their measured elastic differential cross-sections at $E_i = 6$–50 eV. The measurements were done for scattering angles 10–120 degrees and were extrapolated to derive the integrated cross-sections. A comparison in table 3 reveals that the integrated cross-sections of Johnstone and Newell [4] are lower than the present and the other theories, but if the correction ΔQ_{tot} is added (along with inelastic contribution) to the reported measurements, then the theory and the experiment tend to agree. The directly measured Q_{tot} above 50 eV in table 3 are those of Sueoka *et al* [5, 17]. The present results are closer to these measurements also. At 300 eV the agreement is not so good.

3.2 *Differential cross-sections (DCS)*

Vibrationally elastic $e^- - H_2O$ DCS including the dipole-rotation, obtained from our theory are shown in figures 1, 2 and 3 at sample energies 50, 100 and 300 eV respectively. Shown at 50 eV (figure 1) are our theoretical DCS under (i) the complex potential alongwith the dynamically polarized charge-density and (ii) the real potential, with $V_{abs} = 0$. These two calculations differ marginally and agree qualitatively with

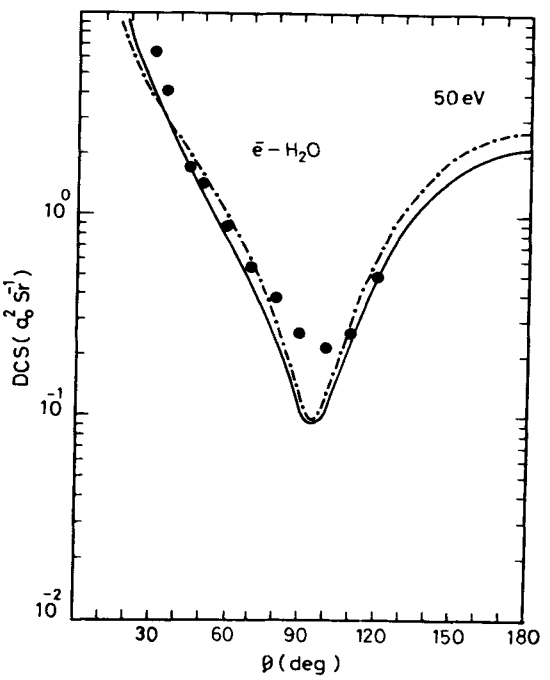

Figure 1. DCS in a_0^2/Sr for $e^- - H_2O$ scattering at 50 eV. ——— present results with dynamically polarized charge-density (complex potential); —·—·— Present results with real potential; ● Experimental DCS of Johnstone and Newell (1991).

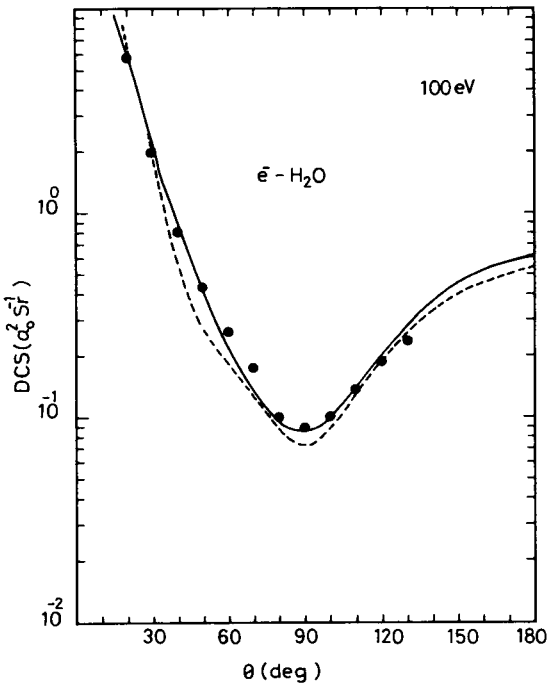

Figure 2. —— Same as in figure 1 but at 100 eV. ---- Present results with statically polarized charge-density (complex potential); ● Experimental DCS of Katase *et al* (1986).

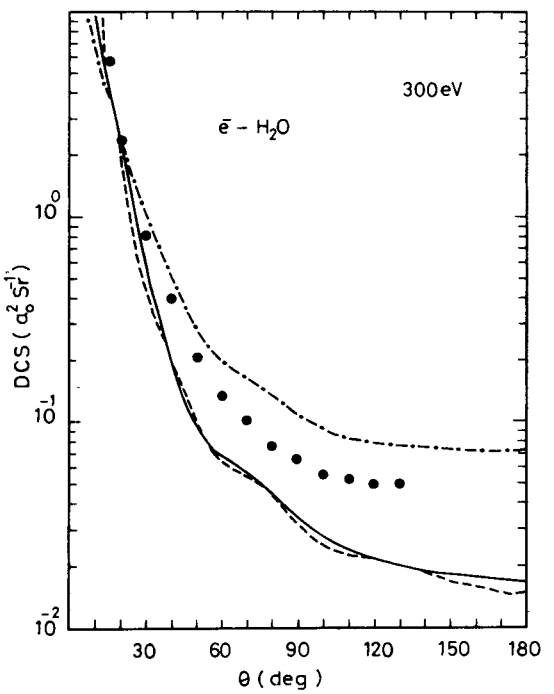

Figure 3. ———— Same as in figure 1 but at 300 eV; ---- Same as in figure 2, but at 300 eV; —·—·—·— Present results with real potential ● Experimental DCS of Katase *et al* (1986).

the experimental DCS of Johnstone and Newell [4]. Our models of (6a) and (6b) do not differ much here. The minimum in the DCS around 100° is deeper in our theory. At 100 eV (figure 2) the present theory, including the dynamical correction (6a) favours the measurements of Katase *et al* [7], better than that with the static correction (6b). Towards high energies the DCS in complex potential, tend to be rather lower at intermediate and large angles. As has been noted earlier [12, 18] this is due to an excessive loss of flux to the inelastic channels, at small r, predicted by the present V_{abs}. We can see from figure 3 (at 300 eV) that the present DCS in the complex potential are lower than the measured DCS of Katase *et al* [7] at intermediate and large angles, while those in the real potential are correspondingly higher. The dynamically polarized charge-density, on which we have focussed attention in this paper, does not appreciably correct this behaviour of the theoretical DCS.

Thus from the present study on $e^- - H_2O$ scattering we conclude the following. The rotational excitation cross-sections, represented through PDFBA are dominant up to about 10 eV and significant even at 100 eV or so, but the present method of calculation, via (1) is satisfactory at intermediate and high energies. The electronically inelastic channels are significant from about 30 eV onwards. The distortion of the target charge-density also assumes significance at these energies, but it should be treated dynamically. An energy-independent polarized charge-density results into overestimation in total cross-sections at high energies. The present Q_{inel} with dynamical distortion, are consistent with the ionization cross-sections. Beyond 300 eV the static charge-density would be sufficient to obtain reliable total cross-sections. Our theoretical DCS are not as good as our total cross-sections. The present absorption potential appears to be rather strong at large E_i and small r.

Acknowledgement

This research was supported in part by the University Grants Commission, New Delhi through a major research project to KNJ.

References

[1] Y Okamoto, K Onda and Y Itikawa, *J. Phys.* **B26**, 745 (1993)
[2] J Yuan and Z Zhang, *Phys. Rev.* **A45**, 4565 (1992)
[3] A Jain, *J. Phys.* **B21**, 905 (1988)
[4] W M Johnstone and W R Newell, *J. Phys.* **B24**, 3633 (1991)
[5] O Sueoka, S Mori and Y Katayama, *J. Phys.* **B19**, L373 (1986)
[6] Y Itikawa, *J. Phys. Soc. Jpn.* **32**, 217 (1972)
[7] A Katase, K Ishibashi, Y Matsuomoto, T Sakae, S Maezono, E Murakami, K Watanabe and H Maki *J. Phys.* **B19**, 2715 (1986)
[8] S Hara, *J. Phys. Soc. Jpn.* **22**, 710 (1967)
[9] G Staszewska, D Schwenke, D Thirumalai and D G Truhlar, *Phys. Rev.* **A28**, 2740 (1983)
[10] N T Padial and D W Norcross *Phys. Rev.* **A29**, 174 (1984)
[11] K N Joshipura and P M Patel, *Pramana – J. Phys.* **38**, 329 (1992)
[12] K N Joshipura and P M Patel, *Phys. Rev.* **A48**, 2464 (1993)
[13] L A Collins and D W Norcross, *Phys. Rev.* **A18**, 467 (1978)
[14] S P Khare and W J Meath, *J. Phys.* **B20**, 2101 (1987)
[15] J Orient and S K Srivastava, *J. Phys.* **B20**, 3923 (1987)
[16] M V V S Rao, (Private Communication) (1994)
[17] O Sueoka, S Mori and Y Katayama, *J. Phys.* **B20**, 3237 (1987)
[18] A Jain, *Phys. Rev.* **A34**, 3707 (1986)